Journal of Chromatography, 608 (1992) 97–107
Elsevier Science Publishers B.V., Amsterdam

CHROM. 24 213

Theoretical and experimental aspects of indirect detection in capillary electrophoresis

Gerard J. M. Bruin, Arian C. van Asten, Xiaoma Xu and Hans Poppe

Laboratory for Analytical Chemistry, University of Amsterdam, Nieuwe Achtergracht 166, 1018 WV Amsterdam (Netherlands)

ABSTRACT

Theoretical and experimental aspects of indirect UV detection are considered. Based on a mathematical treatment of the transport of ions through the capillary, resulting in an eigenvector–eigenvalue problem, some guidelines are formulated about how to increase efficiency and sensitivity in an indirect (UV) detection system. Also, the existence of system peaks can be explained properly. An experimental system consisting of seven amino acids as sample ions and salicylate at pH 11.0 as the UV-absorbing ion was chosen in order to compare theoretical and experimental results. Constructed electropherograms, produced with a computer program based on the above-mentioned mathematical treatment, are also presented and compared with experimental electropherograms.

INTRODUCTION

Most capillary electrophoretic separations are performed using UV detection. Although on-column UV detection requires some degree of miniaturization, it is easy to carry out and is inexpensive. Another important advantage of UV detection is its more or less universal character: peptides, proteins and oligonucleotides can all be detected. However, important classes of compounds such as inorganic ions, amino acids and sugars cannot be detected with UV methods. Indirect detection can be used as a universal detection scheme, without the need for time-consuming precolumn derivatization or experimentally complicated postcolumn derivatization procedures.

The possibilities for indirect laser-induced fluorescence detection have been studied by Yeung and co-workers. They reported successful separations of amino acids [1], proteins, nucleotides [2], tryptic digests [3], sugars [4] and inorganic ions [5]. Detection of aliphatic alcohols and some phenolic compounds separated by micellar electrokinetic capillary chromatography (MECC) in combination with indirect fluorescence detection has been accomplished by Amankwa and Kuhr [6]. The detection mechanism involves a combination of displacement of the fluorescent background ion from the micelle by the sample ion and a net reduction of the quantum efficiency of the fluorophore in the sample zone. Another mode of indirect detection, indirect amperometric detection, has been demonstrated by Olefirowicz and Ewing [7] for the detection of several amino acids and dipeptides.

Indirect UV detection in CZE has been applied for the detection of homologous organic acids and inorganic ions [8–10] and alkylsulphate surfactants [11]. The possibilities for indirect UV detection in MECC systems have been shown recently by Szücs *et al.* [12]. They added sodium dodecylbenzenesulphonate to the buffer, which allowed the detection of neutral, aliphatic alcohols.

Foret *et al.* [10] argued that the highest sensitivity can be achieved for sample ions having a mobility close to that of the UV-absorbing ion. They also gave some calculations on one of the disadvantages of indirect UV detection, the limited linear range (only two orders of magnitude) under favourable

Correspondence to: Professor H. Poppe, Laboratory for Analytical Chemistry, University of Amsterdam, Nieuwe Achtergracht 166, 1018 WV Amsterdam, Netherlands.

0021-9673/92/$05.00

conditions. The upper limit is badly influenced by concentration overload. This effect can be diminished by choosing conditions such that the effective mobilities of the background electrolyte (BGE) and sample ions do not differ too much.

In this paper we treat the theoretical background of the electrophoretic transport in analytical separations in detail by using a mathematical analysis of the transport equation. This treatment consists of a vector–matrix approach which allows the assignment of the various sample and buffer constituents into a set of eigenvectors with corresponding eigenvalues, representing mobilities.

Also, results of the use of a computer program are presented. It predicts the number and position of system peaks with associated mobilities, the peak widths of sample ions, effective mobilities of sample ions at various pH values and the disturbances of the concentrations of the (UV-absorbing) background ions after injection. The results of the computational calculations are compared with experimental results.

The applicability of indirect UV detection in high-performance capillary electrophoresis (HPCE) is demonstrated with a system, consisting of salicylate as the UV-absorbing anion and seven amino acids as sample constituents.

THEORY

In indirect detection, a detectable ion is chosen as one of the components of the background electrolyte (BGE), thus creating a large background signal. When a non-detectable analyte ion passes the detection window, there will be an increase or decrease in concentration of the detectable ion in the analyte zone, resulting in either an increase or decrease in the background signal. For a good description of such systems, one has to start with the fundamental transport equations as has been done for high-performance liquid chromatography (HPLC) by Crommen *et al.* [13]. Poppe [14] showed that the mathematical approaches for the description of indirect detection in HPLC and HPCE are analogous. However, in HPCE the model is simpler. In HPLC the simultaneous distribution of analytes towards the stationary phase has to be characterized empirically in order to arrive at predictions of indirect responses. In HPCE, the system consists of only one phase, while the laws governing coupled transport are unambiguous and well known.

In this mathematical treatment, the following assumptions are made: the injection plug is infinitely sharp; diffusion is neglected, which omits the mass flux, caused by diffusion; no distribution phenomena are involved; and the electro-osmotic flow is zero. These restrictions can be relaxed later on in the model.

We start with Fick's law:

$$\frac{\partial c_i}{\partial t} = -\frac{\partial}{\partial z} \cdot J_i \tag{1}$$

where J_i and c_i are the mass flux and concentration of component i, respectively, and z the coordinate along the axis of the capillary.

The mass flux can be written as

$$J_i = v_i c_i = \mu_i E_z c_i = \frac{j \mu_i c_i}{\gamma} \tag{2}$$

where v_i and μ_i are the linear velocity and the effective mobility, respectively, of compound i, j the current density and γ the specific conductivity; μ_i is a signed quantity and E_z is the local electric field ($= j/\gamma$). The specific conductivity at position z in the capillary can be expressed as

$$\gamma = \mathscr{F} \sum_i z_i \mu_i c_i \tag{3}$$

where $\mathscr{F}$ is the Faraday constant and z_i the charge of the ion.

Combining eqns. 1 and 2 gives

$$\frac{\partial c_i}{\partial t} = -j \cdot \frac{\partial}{\partial z}\left(\frac{\mu_i c_i}{\gamma}\right) \tag{4}$$

From this, it follows that the transport of one ion depends on the concentration of other ions present in the system. For a set of N components, $N-1$ such equations can be found. We need only $N-1$ equations because the concentration of the Nth ion is determined by the electroneutrality.

The set of $N-1$ coupled non-linear equations is too complex to solve; only in a limited number of simple systems is it possible to find solutions. If the disturbance of the concentration of the ions in the background electrolyte is relatively small, then it is allowed to create a set of linear equations. The right-hand side of eqn. 4 can be written as

$$\frac{\partial}{\partial z} \cdot \frac{\mu_i c_i}{\gamma} = \frac{\mu_i}{\gamma} \cdot \frac{\partial c_i}{\partial z} + \mu_i c_i \cdot \frac{\partial}{\partial z} \cdot \frac{1}{\gamma} + \frac{c_i}{\gamma} \cdot \frac{\partial \mu_i}{\partial z} \quad (5)$$

The current density j can be omitted, because it is a constant for a uniform capillary. Both the conductivity, γ, and the mobilities of the ions, μ_i, are functions of the $N-1$ components in the system:

$$\frac{1}{\gamma} = F_1(c_1, c_2, \ldots, c_{N-1}) = \frac{1}{\left(\mathcal{F} \sum_{i=1}^{N-1} z_i \mu_i c_i\right)} \quad (6)$$

$$\mu_i = F_2(c_1, c_2, \ldots, c_{N-1}) \quad (7)$$

The dependence of the μ_is on the electrolyte concentration is a result of ionic strength effects and varying extents of dissociation of acids and bases. Although the latter effects can be handled [15], in this paper we shall treat the μ_is as constants, which means that eqn. 7 needs no further consideration. The partial derivative of eqn. 5 can be expanded as

$$\frac{\partial F}{\partial z} = \frac{\partial F}{\partial c_1} \cdot \frac{\partial c_1}{\partial z} + \frac{\partial F}{\partial c_2} \cdot \frac{\partial c_2}{\partial z} + \ldots + \frac{\partial F}{\partial c_{N-1}} \cdot \frac{\partial c_{N-1}}{\partial z} \quad (8)$$

If eqn. 8 is used to calculate the partial derivative of eqn. 5, the following expression will be obtained:

$$\frac{\partial}{\partial z} \cdot \frac{\mu_i c_i}{\gamma} = \sum_{k=1}^{N-1} A_{i,k} \cdot \frac{\partial c_k}{\partial z} \quad (9)$$

where

$$A_{i,k} = \frac{\partial}{\partial c_k}\left(\frac{\mu_i c_i}{\gamma}\right) \quad (10)$$

This means that eqn. 4 can be rewritten as

$$\frac{\partial c_i}{\partial t} = -\sum_{k=1}^{N-1} A_{i,k} \frac{\partial c_k}{\partial z} \quad (11)$$

for ions $i = 1, \ldots, N-1$.

In vector–matrix notation, eqn. 11 is

$$\frac{\partial}{\partial t} \cdot \bar{c} = |A| \cdot \frac{\partial}{\partial z} \cdot \bar{c} \quad (12)$$

If there is only one compound in the system, there is also only one differential equation and then the solution is easy to find:

$$c = G(z - \lambda t) \quad (13)$$

where λ is a constant (with the units of velocity) and $G'(x)$ a function, *e.g.*, the injection profile. This solution means that the injection pulse occurring in the capillary at $t = 0$ is transported through it with velocity λ without deformation. A representation of this can be found in Fig. 1A. In reality there is always more than one component in the system, which results in a set of coupled linear equations. This more-dimensional problem can be solved if it is possible to find a set of simultaneously occurring, concerted disturbances in all concentrations, which remain unchanged during transport along the capillary. An example of the situation for a three-ion system at $t = 0$ and $t = t$ is depicted in Fig. 1B. The system consists of a sample ion A^+, which is electrophoresed in a BGE B^+C^-. For a more-ions system, this can be represented mathematically as

$$\begin{aligned} c_1 &= e_1 G(z - \lambda t) \\ &\cdot \\ &\cdot \\ &\cdot \\ c_{N-1} &= e_{N-1} G(z - \lambda t) \end{aligned} \quad (14)$$

where e_1 to e_{N-1} indicate the relative intensity of the disturbance of the concentration. If the changes in

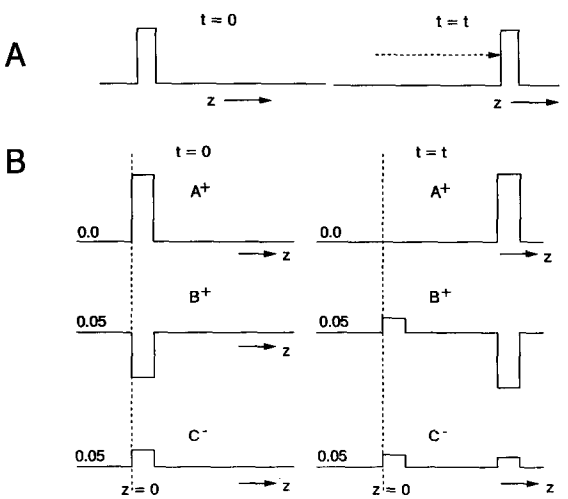

Fig. 1. Schematic representation of disturbances of the concentrations of the components after injection. The zones with the concerted concentration disturbances travel with a fixed velocity λ through the capillary. (A) One-dimensional system; (B) more-dimensional system. Sample ion A^+ is electrophoresed in B^+C^-. The numbers on the z-axis indicate the ion concentration. Note also the stagnant zone at $z = 0$ in case of $t = t$. This zone is nearly always visible in indirect detection measurements as a system peak at the position of an electroosmotic flow marker.

the concentrations as described above are substituted in the set of coupled linear equations, the result is

$$e_i \cdot \frac{\partial G}{\partial t} = -\sum_{k=1}^{N-1} [A_{i,k} e_i] \frac{\partial G}{\partial z} \quad (i = 1, \ldots, N-1) \qquad (15)$$

The term in between brackets does not depend on time and position in the capillary.

The set can only be solved if the concerted disturbances of the various concentrations in the zone migrate at the same velocity. These disturbances can be indicated as eigenpeaks with an associated eigenvalue λ, representing the velocity. The terms in brackets in eqn. 15 can be expressed as

$$-\sum_{k=1}^{N-1} [A_{i,k} e_k] = -\lambda e_i \quad (i = 1, \ldots, N-1) \qquad (16)$$

This gives rise to the following eigenvalue problem in matrix notation:

$$|A|\bar{e} = \lambda \bar{e} \qquad (17)$$

To demonstrate the theoretical treatment above, we use a simple example of the electrophoresis of an amino acid, glycine (gly), in a BGE of sodium salicylate (referred to in the equations as Na and sal). This example was chosen because it shows a resemblance with the experimental part as described in this paper.

It will be assumed here that the ions are not subject to acid–base equilibria. This assumption leads to a fixed effective mobility. In this paper mobilities are always indicated as "overall" when they include the electroosmotic migration and as effective when the effects of acid–base reactions have been taken into account. The A term is now

$$A_{i,k} = \mu_i \cdot \frac{\partial}{\partial c_k}\left[\frac{c_i}{\gamma}\right] = \mu_i \left[c_i \cdot \frac{\partial}{\partial c_k}\left(\frac{1}{\gamma}\right) + \frac{1}{\gamma} \cdot \frac{\partial c_i}{\partial c_k}\right] \qquad (18)$$

The Na^+ ion is selected here as the dependent ion; the concentration is not explicitly given, but can be calculated easily from the rules of electroneutrality in the zone; c_{gly} and c_{sal} are taken as the independent variables. The conductivity in this electrophoretic system is

$$\gamma = c_{gly}[\mu_{Na} - \mu_{gly}] + c_{sal}[\mu_{Na} - \mu_{sal}] \qquad (19)$$

Combining eqns. 18 and 19 results in

$$A_{gly,gly} = \frac{\mu_{gly}}{\gamma} - \frac{\mu_{gly} c_{gly}[\mu_{Na} - \mu_{gly}]}{\gamma^2} \approx \frac{\mu_{gly}}{\gamma} \quad (c_{gly} \approx 0) \qquad (20)$$

$$A_{gly,sal} = -\frac{\mu_{gly} c_{gly}[\mu_{Na} - \mu_{sal}]}{\gamma^2} \approx 0 \quad (c_{gly} \approx 0) \qquad (21)$$

$$A_{sal,gly} = -\frac{\mu_{sal} c_{sal}[\mu_{Na} - \mu_{gly}]}{\gamma^2} \qquad (22)$$

$$A_{sal,sal} = \frac{\mu_{sal}}{\gamma} - \frac{\mu_{sal} c_{sal}[\mu_{Na} - \mu_{sal}]}{\gamma^2} \approx 0 \quad (c_{sal}[\mu_{Na} - \mu_{sal}] \approx \gamma) \qquad (23)$$

The matrix equation is therefore

$$\begin{vmatrix} \frac{\mu_{gly}}{\gamma} & 0 \\ -\frac{\mu_{sal} c_{sal}[\mu_{Na} - \mu_{gly}]}{\gamma^2} & 0 \end{vmatrix} \begin{vmatrix} c_{gly} \\ c_{sal} \end{vmatrix} = \lambda \begin{vmatrix} e_{gly} \\ e_{sal} \end{vmatrix} \qquad (24)$$

There are two solutions,

$$\lambda_1 = \frac{\mu_{gly}}{\gamma} \Rightarrow \frac{e_{sal}}{e_{gly}} = -\frac{\mu_{sal}}{\mu_{gly}} \cdot \frac{(\mu_{Na} - \mu_{gly})}{(\mu_{Na} - \mu_{sal})} \qquad (25)$$

$$\lambda_2 = 0 \Rightarrow e_{gly} = 0 \qquad (26)$$

The first solution corresponds to the electrophoresis of glycine with the associated disturbance in the salicylate concentration, expressed as e_{sal}/e_{gly}, in the sample zone; e_{sal}/e_{gly} is defined here as the response factor. Salicylate now allows us to monitor the passing non-UV-absorbing ion, glycine, by its change in concentration as a consequence of the presence of this glycine in the zone. It is noteworthy that the disturbance is not a direct consequence of electroneutrality rules; this would give $e_{gly} = -e_{sal}$, which is only true when $\mu_{gly} = \mu_{sal}$. In that particular situation, there will be a one-to-one displacement.

The second solution has velocity $\lambda = 0$, which will be visualized as a system peak, because it will be transported by the electroosmotic flow (if present). (The existence of such a stagnant concentration disturbance was discussed already in 1967 by Hjertèn [16].) This stagnant zone serves as a very effective electroosmotic flow marker in this way. In Fig. 1B, this zone is depicted at $z = 0$ and $t = t$.

The Kohlrausch regulating function (KRF),

which cannot change with time, should be fulfilled at all times for the moving sample zone. This can be checked by applying the KRF to the disturbances in the zone. The change in concentration of Na^+, e_{Na}/e_{gly}, can be calculated from electroneutrality:

$$\frac{e_{sal}}{e_{gly}} - \frac{e_{Na}}{e_{gly}} + 1 = 0 \Rightarrow \frac{e_{Na}}{e_{gly}} = 1 + \frac{e_{sal}}{e_{gly}} \quad (27)$$

The term in the KRF caused by the disturbance is

$$\Delta KRF = \sum_i \left[\frac{(\Delta c_i)z_i}{\mu_i}\right]$$

$$= -\frac{1}{\mu_{gly}} - \frac{e_{sal}/e_{gly}}{\mu_{sal}} + \frac{(1 + e_{sal}/e_{gly})}{\mu_{Na}} \quad (28)$$

Combining eqn. 27 and the expression for e_{sal}/e_{gly} (eqn. 25) results in $\Delta KRF = 0$, so that the zone is indeed allowed to move through the capillary.

For the description of this simple three-component system, it is not absolutely necessary to use the eigenvector–eigenvalue treatment; the same results can be obtained by applying the Kohlrausch function and the rules for electroneutrality. However, when more than two components are involved in the BGE and/or the ions possess dissociation constants, one has to use the eigenzone treatment with suitable refinement, in which also $d\mu/dpH$ is allowed for [15].

EXPERIMENTAL

Instrumentation

The experimental apparatus used was laboratory built and essentially the same as described previously [17]. All the indirect UV detection measurements were done at 234 nm. For this wavelength also a calibration graph for salicylate was measured in the same way as previously described [18]. The capillary detection cell was laboratory made and has an adjustable slit. In all experiments, capillaries of I.D. 50 μm and O.D. 350 μm were used (Polymicro Technologies, Phoenix, AZ, USA). The slit in front of the detection window was adjusted to an aperture width of 50 μm, which gives an optimum signal-to-noise ratio for this type of detection cell [18]. Separations in which potassium chloride was added to the buffer were carried out on a prototype PRINCE (programmable injector for capillary electrophoresis) from Lauer Labs. (Emmen, Netherlands) in combination with a FUG (Rosenheim, Germany) high-voltage power supply and a Spectra-Physics (Eindhoven, Netherlands) UV detector. This equipment allowed both accurate electrokinetic and pressure injection.

Separations were performed in 5 and 10 mmol/l salicylate solutions in a capillary with a total length of 59.0 cm and a length from the injection to detection point of 36.0 cm. Injection was done by electromigration at 6 kV for 5 s. The separation voltage was 15 kV with recorded currents between 5.0 and 5.2 μA. The temperature in the air-thermostated safety box was 24.0 ± 0.2°C (unless stated otherwise). In some experiments, KCl or 3-cyclohexylamino-1-propanesulphonic acid (CAPS) was added to the background electrolyte to study the influence of the ionic strength on plate number, sensitivity and concentration overload.

UV spectra of $1 \cdot 10^{-4}$ mol/l sodium salicylate were measured with a Philips PU 8720 UV–VIS scanning spectrophotometer, using quartz cuvettes with an optical path length of 1 cm.

Chemicals

Sodium salicylate and CAPS were obtained from Aldrich, valine and serine from Nutritional Biochemical, lysine, glutamic acid and sodium chloride from Merck, proline from Janssen Chimica and alanine from P-L Biochemicals.

RESULTS

The application of indirect UV detection has been demonstrated with the separation of seven amino acids (listed in Table I) at pH 11, ranging in concentration from $5 \cdot 10^{-3}$ to $1 \cdot 10^{-3}$ mol/l and dissolved in the BGE. Working at this high pH was necessary to give the amino acids a net negative charge and different electrophoretic mobilities. From Table I, it can be seen that the majority of the amino acids (except proline) are nearly 100% dissociated at pH 11.0. Glutamic acid is doubly negatively charged as a result of the second carboxyl group in the molecule.

In Fig. 2A and B some typical electropherograms obtained with this system are depicted. In Fig. 2A, the salicylate concentration in the background electrolyte (BGE) was 5 mmol/l and in Fig. 2B 10 mmol/l. The sample concentration of each amino

TABLE I

DISSOCIATION CONSTANTS, MEASURED ELECTROPHORETIC MOBILITIES AND RELATIVE STANDARD DEVIATIONS AND RESPONSE FACTORS FOR THE AMINO ACIDS

For experimental conditions, see text.

Amino acid	pK_a	μ_{eff}[a]		Response factor[b]
		Value (10^{-5} cm^2/V · s)	R.S.D. (%)	
Proline	10.64	−16.8	1.2	1.044
Leucine	9.74	−23.0	0.6	1.191
Valine	9.74	−24.6	0.8	1.144
Alanine	9.92	−28.0	0.7	1.029
Serine	9.26	−29.5	0.5	1.073
Glycine	9.96	−32.6	0.4	0.937
Glutamic acid	9.96	−44.3	0.5	1.738
Salicylic acid[c]	3.11	−35.4		

[a] The mobilities are the mean values of six analyses.
[b] The response factors are calculated by the computer program, based on the theory as described.
[c] Values taken from ref. 19.

acid was 1 mmol/l in both instances. These electropherograms show again that indirect detection offers good possibilities for the detection of non-absorbing ions, in agreement with earlier papers by others [8–11]. The concentration detection limits are close to 10^{-5} mol/l for this separation and detection system, which is in the same range as for normal HPCE with UV detection systems.

As discussed in the theoretical section, a large system peak can be observed in the electropherogram, which migrates with the electroosmotic velocity. The last eluting peak with the lowest overall mobility is glutamic acid, because it is double negatively charged and thus travels with the highest effective mobility, against the electroosmotic flow. The first appearing peak corresponds to proline. Proline, having a high pK_a value (see Table I), is only partly dissociated at pH 11.0, which causes the effective, electrophoretic mobility to be the smallest. This amino acid is very sensitive to small pH changes; for instance, a pH change from 11.0 to 10.8 gives a 15% reduction in electrophoretic mobility, whereas the reduction for the other amino acids is only between 1 and 3%. This is also an explanation for the observed higher relative standard deviation

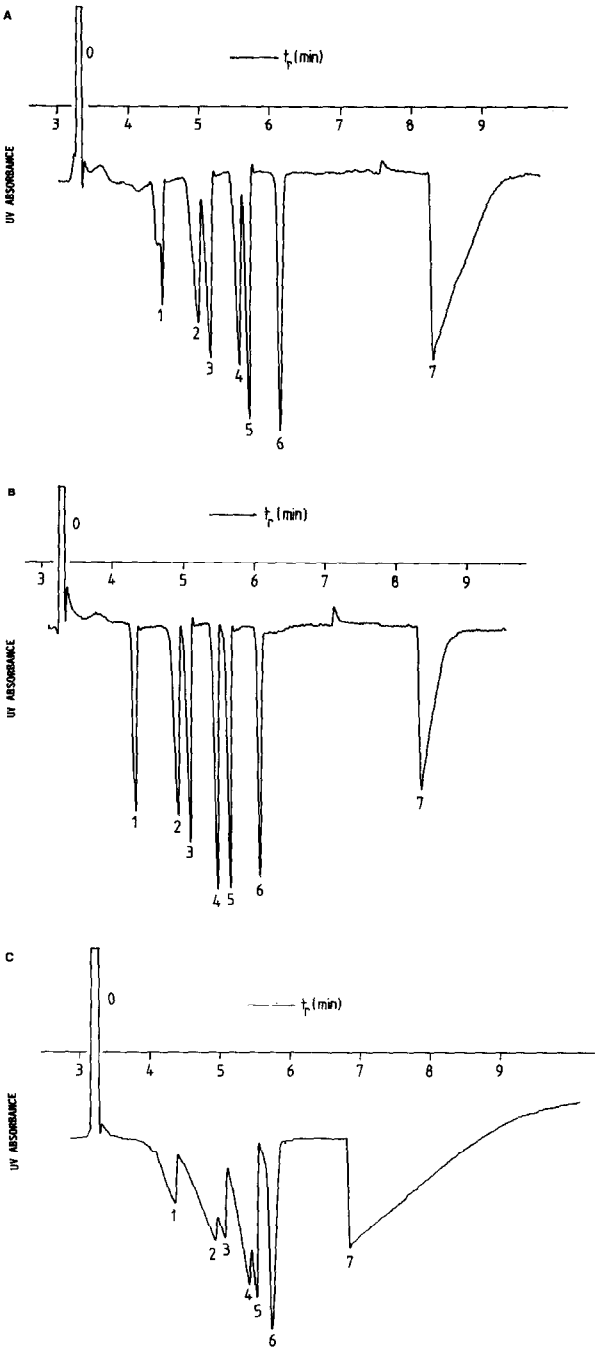

Fig. 2. Electropherograms of the separation of (1) proline, (2) leucine, (3) valine, (4) alanine, (5) serine, (6) glycine and (7) glutamic acid. Background electrolyte: sodium salicylate, pH 11.0. (A) 5 and (B) 10 mmol/l. Injection: 1 mmol/l of each amino acid. (C) Injection of 5 mmol/l of each amino acid, BGE = 5 mmol/l salicylate. For further experimental conditions, see text.

of the measurements of the electrophoretic mobility for this amino acid (Table I).

Overload can be very severe in indirect detection systems [16]. The peak deformation increases at higher sample concentrations and results in a loss of efficiency. This effect depends strongly on the sample/buffer concentration ratio, as can be seen in Fig. 2A and B. In Fig. 2A, the concentration overload, as witnessed by the triangular shape, is much stronger than in Fig. 2B, where 10 mmol/l was used. The experimentally determined effective mobilities of proline, leucine, valine, alanine and serine are smaller than the effective mobility of salicylate (see Table I). This results in fronting peaks, which is more pronounced when the sample/BGE concentration ratio increases. The electrophoretic mobility of glutamate is larger (more negative), resulting in badly tailing peaks [20]. The electrophoretic mobility of glycine nearly equals that of salicylate, which is why the conductivity of the glycine zone will not differ much from the BGE conductivity and peak deformation can be avoided. This is clearly illustrated in Fig. 2C, where 5 mmol/l of each amino acid was injected in a 5 mmol/l salicylate carrier. With this extreme example of concentration overload, only glycine still has a more or less Gaussian peak shape. In Table I, the effective mobilities of the amino acids and their relative standard deviations (R.S.D.s) are given. Except for proline, all the R.S.D.s are below 1%.

In Fig. 3, a graph of the plate number *N versus* the electrophoretic mobilities of the amino acids is shown. It clearly demonstrates the above-mentioned effects with higher plate numbers for peaks having a mobility close to that of the background ion. It is noteworthy that the difference in plate number for 1 and 0.1 mmol/l glycine injection is smaller than for the other amino acids. This can be attributed to the smaller zone deformation for glycine, as explained earlier. The same trends as in Fig. 3 can be found for the situation with 10 mmol/l salicylate in the BGE. The plate numbers are higher, between 70 000 and 120 000 for injection of 10^{-4} mol/l of each amino acid, because the effect of concentration overload is less pronounced.

To obtain an even better performance in this respect, one approach could be to increase the salicylate concentration further. Provided that the tube diameter is not too large and excessive heat dissipation can be avoided, this would certainly

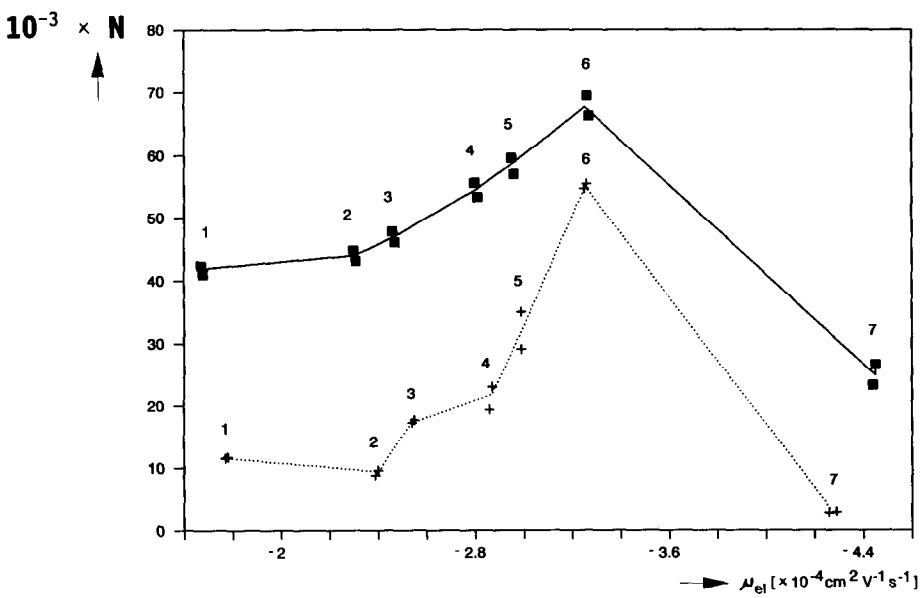

Fig. 3. Plate number *versus* electrophoretic mobility of the amino acids for two sample concentrations: solid line, 10^{-4} mol/l amino acid; dotted line, 10^{-3} mol/l amino acid. Numbers on the graphs correspond to those in Fig. 2.

improve the separation performance. However, indirect detection is likely to be adversely affected under such conditions, for two reasons. First, the UV absorbance signal turns out to be severely non-linear at salicylate concentrations above 0.01 mol/l, a result of optical non-idealities such as non-uniform path length and stray light. Hence, although the replacement ratio salicylate/sample ion will be virtually the same, the response in experimental absorbance units decreases, leading to a poorer signal-to-noise ratio. The above-mentioned effect is illustrated in Fig. 4, where peak area is plotted *versus* alanine concentration. Smaller peak areas are found for a BGE concentration of 10 mmol/l. It must be noted that as a result of manual electrokinetic injection and manual triangulation of peak areas to determine the area, the accuracy is less than that with an automated injection device.

Second, this degradation of the signal-to-noise ratio is amplified by the increase in noise at the high absorbance values occurring in most photometers. For instance, assuming a constant noise level, σ_I, in the intensity (I) measurement, the conversion to absorbance units, A, would give a noise level, σ_A, of

$$\sigma_A = 0.4343 \frac{\sigma_I}{(I/I_0)} = 0.4343\sigma_I \cdot 10^A \qquad (29)$$

which would predict a tenfold higher noise level at $A = 1$. Most UV detectors do not have a constant σ_I value; the σ_I value rather increases with I, with an exponent between 0.5 (shot noise-limited case) and 1.0 (source instability-limited case). For shot noise limitation one would obtain σ_A = constant · $10^{0.5A}$ instead of eqn. 29. As indeed (partial) shot noise limitation (*i.e.*, source intensity limitation) is most common, an incraese in σ_A with A can still be expected, although less severe than predicted by eqn. 29.

Preliminary experiments confirmed these expectations, so that the approach of higher salicylate concentration was abandoned.

Another approach would be to increase the ionic strength of the BGE by adding a buffer or a salt. This was tested by adding various concentrations of KCl to the sodium salicylate solution in both the BGE and the sample. In Fig. 5, the peak area of alanine is plotted *versus* KCl concentration. The salicylate concentration was kept constant at 5 mmol/l. Increasing the KCl concentration to 25 mmol/l resulted in a decrease in sensitivity by a factor of 2 (the peak area for alanine with 50 mmol/l in the BGE could not be determined properly, because of increasing thermal noise with increasing KCl concentration). The smaller sensitivity can be attributed to the decrease in the ratio e_{sal}/e_{ala} (eqn. 25) (see the next section). As can be seen in Fig. 5, there is no large difference between pressure injection and electrokinetic injection. For the electrokinetic injection the integrated peak area is larger because of the longer injection plug in this instance. When pressure injection was applied the integrated area had to be

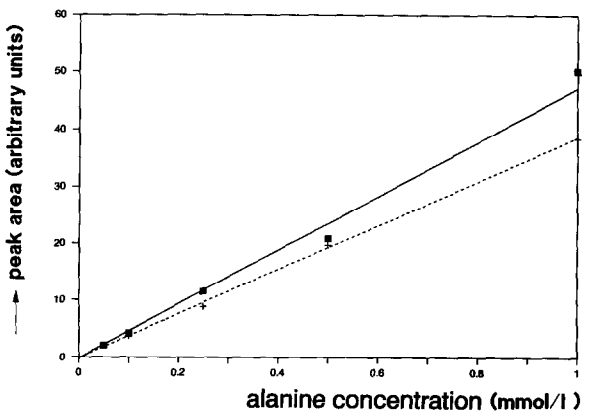

Fig. 4. Peak area *versus* alanine concentration. For experimental conditions, see text. Salicylate concentration: solid line, 5 mmol/l; dashed line, 10 mmol/l.

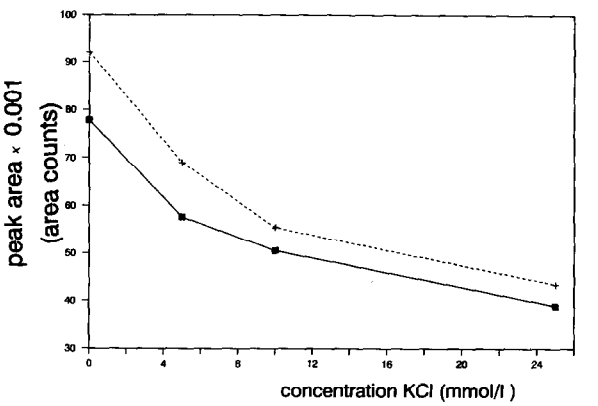

Fig. 5. Peak area of alanine *versus* KCl concentration. Injection of 0.1 mmol/l alanine dissolved in BGE (5 mmol/l salicylate, pH 11.0). Solid line, pressure injection, ΔP = 80 mbar, t_{inj} = 1.8 s; dashed line, electrokinetic injection, 6 s, 6000 V. L = 59.0 cm; $l_{inj-det}$ = 41.5 cm; voltage, 15 000 V; T = 30.0°C.

TABLE II

CALCULATED RESPONSE FACTOR OF THE ALANINE PEAK AND MEASURED ELECTROOSMOTIC MOBILITY AS A FUNCTION OF KCl CONCENTRATION

Conditions used as input for the computer program: BGE, 5 mmol/l sodium salicylate, adjusted to pH 11.0 with sodium hydroxide. Absolute mobilities (10^{-5} cm^2/V · s) for the cations and anions: $\mu(K^+) = 76.2$, $\mu(Na^+) = 51.9$, $\mu(Cl^-) = 78.83$ (all taken from ref. 21), μ(salicylate) = −35.4, pK_a = 3.1 (ref. 19); μ(alanine) = −30.33 (experimentally determined), pK_a = 9.92.

[KCl] (mmol/l)	Response factor	$10^5\mu_{eo}$ (cm^2/V · s)
0	1.029	86.6
5	0.863	77.4
10	0.742	72.2
25	0.523	64.9
50	0.351	59.8

corrected by a factor t_{ala}(BGE1)/t_{ala}(BGE2), where t_{ala} is the migration time of the alanine zone. This correction has to be made in order to compensate for the decreased electroosmotic flow (see Table II) at higher ionic strength, which should give too high a peak area compared with the situation without KCl in the BGE. The correction can be omitted with electrokinetic injection, because one also injects less at higher ionic strength; the injection volume is smaller by the same correction factor. Here, the reduced injection volume and larger integrated area cancel. In Fig. 6, the observed plate numbers are

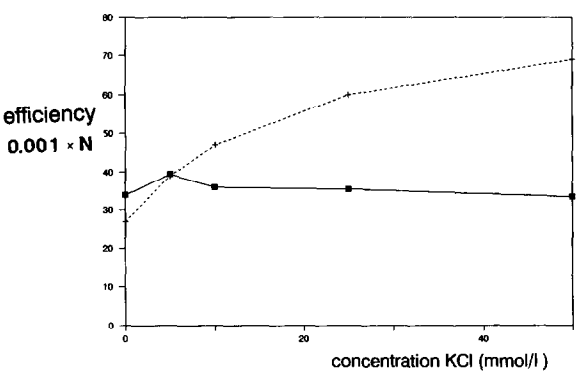

Fig. 6. Effect of KCl concentration on the efficiency of the alanine peak. Injection of 0.1 mmol/l alanine. Salicylate concentration = 5 mmol/l. Dashed line, electrokinetic injection; solid line, pressure injection. Experimental conditions as in Fig. 5.

plotted as a function of the KCl concentration. The efficiency increases from 27 000 plates at zero KCl content to 69 000 plates at 50 mmol/l KCl for an electrokinetic injection of $1 \cdot 10^{-4}$ mol/l alanine. This gain in efficiency can be attributed to a combined effect of a smaller contribution from concentration overload and injection volume. In pressure injection, the efficiency is constant, because here the injection volume is the predominant source of zone broadening.

Buffering with CAPS, a zwitterion with a low mobility and buffering capacity at high pH, will contribute little to the conductivity of the BGE. This is expected to have a small negative effect on the sensitivity, whereas the stability of the indirect detection system will be increased. However, measurements showed that adding CAPS resulted in a threefold decrease in sensitivity (depending on the CAPS concentration). Also, an extra system peak with $\mu_{el} = -18 \cdot 10^{-5}$ cm^2/V · s appeared in the electropherogram, which partly overlapped the proline peak.

Computer simulation of indirect detection

The theory described has been implemented in a computer program. The program itself and the possibilities are treated more into detail elsewhere [15]. The computer program can be a valuable tool to gain some insight into the ionic strength and conductivity of BGEs, the degree of peak deformation due to concentration overload, the response when indirect detection is used and the position and number of system peaks in the electropherogram.

The details of peak construction are also explained in detail elsewhere [15]. Usually, only two points of a peak are evaluated, one at zero sample concentration and the other at 10^{-6} mol/l concentration. The difference in mobility represents the dependence of migration time on concentration. This is forced into a linear equation. By applying the mass balance, one can construct a triangle which would be the peak without other dispersive sources. The dispersion term caused by diffusion and injection is added to the width obtained from the nonlinearity equation.

Here, some results from calculations on the response for the seven amino acids and some simulated electropherograms are presented in order to compare them with experimentally obtained

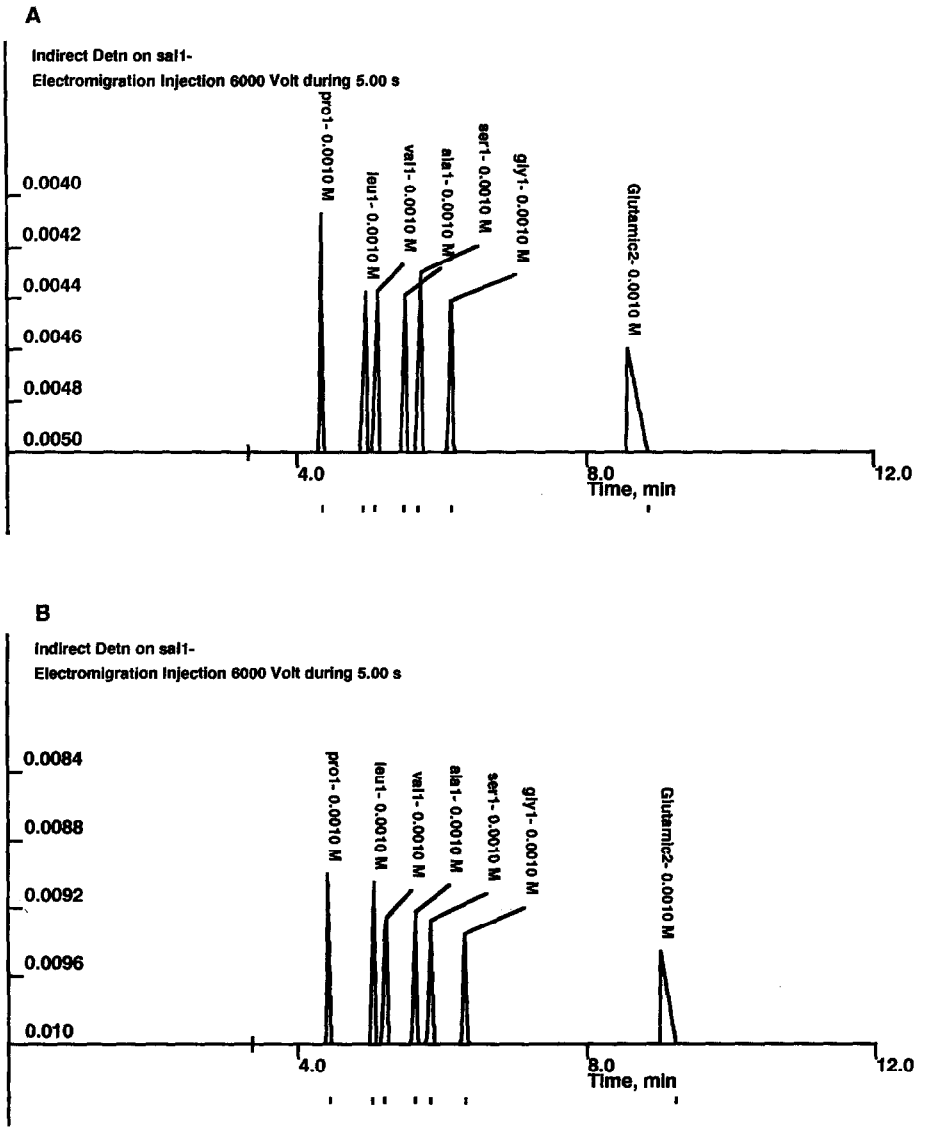

Fig. 7. Constructed electropherograms for two different BGEs at pH 11.0: (A) 5 and (B) 10 mmol/l salicylate. Injection of 10^{-3} mol/l of each amino acid (5 s, 6 kV). $\mu_{eo} = 71.1 \cdot 10^{-5}$ cm^2/V · s; $L = 59.0$ cm; $l_{inj-det} = 36.0$ cm; voltage = 15 000 V. The small vertical line through the time axis corresponds to the position of the system peak.

results. As can be seen in Table I, for the glutamic acid peak the response factor is much larger than for the other amino acids, because of the double charge of this ion. Fig. 7A and B show simulated electropherograms with 5 and 10 mmol/l salicylate (pH 11.0) as the BGE. The fronting and tailing of the peaks, depending on the electrophoretic mobilities relative to the salicylate mobility, are well predicted: fronting for the first five peaks, glycine with a reasonable gaussian shape and glutamic acid eluting with a tailing peak shape. The small vertical line through the time axis corresponds to the position of the system peak.

Also, the dependence of the response factor on the

composition of the BGE was calculated. In Table II the dependence of the response factor of alanine is given as a function of KCl concentration, the salicylate concentration being kept at 5 mmol/l. As can be seen, there is a decrease (by a factor of three) in sensitivity on going to 50 mmol/l KCl. The same trend was found in the experiment, as can be seen in Fig. 5. A decrease in sensitivity by a factor of 2 was observed at 25 mmol/l KCl, whereas the computer simulation gave a decrease in the response factor (replacement ratio) from 1.029 to 0.523.

CONCLUSIONS

The separation and detection of amino acids is a good demonstration of the applicability of indirect UV detection in HPCE, in which detection limits of the order of 10^{-5} mol/l can be obtained without difficulty. For 5 mmol/l salicylate in the background electrolyte, the sensitivity of the detection system was higher than for 10 mmol/l, because of the non-linearity of the calibration graph of salicylate at higher concentrations in this concentration range. However, a low BGE concentration results in lower efficiencies as a result of the stronger influence of concentration overload at higher sample concentrations. Adding KCl to the BGE diminishes the sensitivity, but increases the separation efficiency.

Adjusting the effective mobility to a value close to that of the background ion is one way to increase both the sensitivity and the efficiency. A problem, occurring regularly, was the instability of this indirect detection system. This could be seen as drift and/or large disturbances of the baseline. Indirect detection is a universal method; all ionic compounds that are present in the sample can be detected in principle, which is why the system is sensitive to impurities.

The simple background electrolyte used throughout this study, sodium salicylate at pH 11.0, has some disadvantages. The BGE has to be refreshed after a few hours of electrophoresis, because the pH shifts to lower values as a result of ion depletion and diffusion of carbon dioxide in the solution.

ACKNOWLEDGEMENT

We thank Dr. Henk Lauer of Lauer Labs. for the loan of a prototype of the programmable injector for CE.

REFERENCES

1 W. G. Kuhr and E. S. Yeung, *Anal. Chem.*, 60 (1988) 2642.
2 W. G. Kuhr and E. S. Yeung, *Anal. Chem.*, 60 (1988) 1832.
3 B. L. Hogan and E. S. Yeung *J. Chromatogr. Sci.*, 28 (1990) 15.
4 T. W. Garner and E. S. Yeung, *J. Chromatogr.*, 515 (1990) 639.
5 L. Gross and E. S. Yeung, *J. Chromatogr.*, 480 (1989) 169.
6 L. N. Amankwa and W. G. Kuhr, *Anal. Chem.*, 63 (1991) 1733.
7 T. M. Olefirowicz and A. G. Ewing, *J. Chromatogr.*, 499 (1990) 713.
8 S. Hjertén, K. Elenbring, F. Kilár, J. Liao, A. J. Chen, C. J. Siebert and M. Zhu, *J. Chromatogr.*, 403 (1987) 47.
9 M. T. Ackermans, F. M. Everaerts and J. L. Beckers, *J. Chromatogr.*, 549 (1991) 345.
10 F. Foret, S. Fanali, L. Ossicini and P. Boček, *J. Chromatogr.*, 470 (1989) 299.
11 M. W. F. Nielen, *J. Chromatogr.*, 588 (1991) 321.
12 R. Szücs, J. Vindevogel and P. Sandra, *J. High Resolut. Chromatogr.*, 14 (1991) 692.
13 J. Crommen, G. Schill, D. Westerlund and L. Hackzell, *Chromatographia*, 14 (1987) 252.
14 H. Poppe, *J. Chromatogr.*, 506 (1990) 45.
15 H. Poppe, *Anal. Chem.*, in press.
16 S. Hjertén, *Chromatogr. Rev.*, 9 (1967) 122.
17 G. J. M. Bruin, R. H. Huisden, J. C. Kraak and H. Poppe, *J. Chromatogr.*, 480 (1989) 339.
18 G. J. M. Bruin, G. Stegeman, A. C. van Asten, X. Xu, J. C. Kraak and H. Poppe, *J. Chromatogr.*, 559 (1991) 163.
19 T. Hirokawa, M. Nishino, N. Aoki, Y. Kiso, Y. Samamoto, T. Yagi and J. Akiyama, *J. Chromatogr.*, 271 (1983) D1–D106.
20 F. E. P. Mikkers, F. M. Everaerts and Th. P. E. M. Verheggen, *J. Chromatogr.*, 169 (1979) 1.
21 J. L. Beckers, Th. P. E. M. Verheggen and F. M. Everaerts, *J. Chromatogr.*, 452 (1988) 591.